HHS Public Access

Author manuscript

Biotribology (Oxf). Author manuscript; available in PMC 2018 June 01.

Published in final edited form as:

Biotribology (Oxf). 2017 June ; 10: 42–50. doi:10.1016/j.biotri.2017.03.006.

In-situ Generated Tribomaterial in Metal/Metal Contacts: current understanding and future implications for implants

N. Espallargas[a], **A. Fischer**[b], **A. Igual Muñoz**[c,d,*], **S. Mischler**[d], and **M.A. Wimmer**[e]

[a]NTNU, Norwegian University of Science and Technology, Faculty of Engineering Science and Technology, Department of Engineering Design and Materials, Tribology Lab, N-7491 Trondheim, Norway [b]University Duisburg-Essen, Institute of Product Engineering, Lotharstr. 1, 47057 Duisburg, Germany [c]UPV, Universitat Politècnica de València, Instituto de Seguridad Industrial, Radiofísica y Medioambiental. Camí de Vera s/n, 46022València [d]EPFL Ecole Polytechnique Fédérale de Lausanne, SCI-STI-SM, 1015 Lausanne, Switzerland [e]Dept. of Orthopedic Surgery, Rush University Medical Center, Chicago IL-60612, USA

Abstract

Artificial hip joints operate in aqueous biofluids that are highly reactive towards metallic surfaces. The reactivity at the metal interface is enhanced by mechanical interaction due to friction, which can change the near-surface structure of the metal and surface chemistry. There are now several reports in the literature about the in-situ generation of reaction films and tribo-metallurgical transformations on metal-on-metal hip joints. This paper summarizes current knowledge and provides a mechanistic interpretation of the surface chemical and metallurgical phenomena. Basic concepts of corrosion and wear are illustrated and used to interpret available literature on in-vitro and in-vivo studies of metal-on-metal hip joints. Based on this review, three forms of tribomaterial, characterized by different combinations of oxide films and organic layers, can be determined. It is shown that the generation of these tribofilms can be related to specific electrochemical and mechanical phenomena in the metal interface. It is suggested that the generation of this surface reaction layer constitutes a way to minimize (mechanical) wear of MoM hip implants.

1 Introduction

Total hip and knee replacements are widely regarded as successful surgical procedures with overall good clinical outcome [1]. This success, coupled with an aging population, has led to a steep increase in procedures during the last decade with currently more than 300,000 primary hips and twice as many knees performed each year in the United States alone [2]. Nearly all of the available joint replacement devices use metal alloys for some parts of the device, especially for the anchoring stems, femoral articulations, and any metal backings of bearing liners, where high strength and fatigue resistance are necessary to guarantee longevity in vivo. The utilized metals are alloys based on cobalt, titanium, and iron, all with excellent passive corrosion characteristics due to an oxide layer that forms spontaneously at

*Corresponding author, anna.igualmunoz@epfl.ch.

the surface. However, absence or damage of the oxide layer causes metal release into the periprosthetic tissue with potentially drastic adverse reactions of the soft tissue. Wear of the joint surfaces is known to introduce damage of the oxide film. Cyclic oxide film removal followed by repassivation leads to corrosion and wear that act in synergy, i.e. a tribocorrosion situation [3–4]. The interaction between wear and corrosion phenomena has been identified as one of the key mechanisms governing the degradation of MoM implants [5]. Quantitative prediction of material loss from MoM bearing surfaces based on tribocorrosion concepts was firstly proposed by Mischler et al. [6]. Cao et al. [7–8] recently developed a comprehensive predictive model considering mechanical wear, wear accelerated corrosion and hydrodynamic lubrication that was able to predict with high precision the degradation of MoM implants in simulators. However, this model does not consider the build-up of tribomaterial as reported in [9–10].

Clinically, this problem surfaced with a group of hip devices using self-mating cobalt-chromium-molybdenum (CoCrMo) alloy bearings with large heads. These so-called metal-on-metal (MoM) joints showed unexpectedly high failure rates due to wear and corrosion alarming the orthopedic industry and clinical community [11–12]. In 2015, the Australian Registry published a failure rate of 22.4% at 10 years for MoM hips with large (>32 mm) head sizes in their report [13]. This is a direct result of the poor mechanistic knowledge of the degradation mechanism(s). Although wear and corrosion have long been recognized as the problem limiting the long-term survival of orthopaedic implants [14], there remains a dearth of knowledge regarding the underlying mechanisms. This is in part due to the extremely complex environment. Within the contact zone of articulating or fretting metal surfaces, there are complex metal-protein compounds that are generated because of the availability of high frictional and/or chemical energy [15].

An understanding of how to utilize synergistic interactions of wear and corrosion towards material protection may provide a leap in safety for future devices that are restricted to materials without suitable alternatives. In this paper, it is reviewed the basic mechanisms and current understanding of metal/metal interaction in the human body with a particular focus on surface transformations occurring on MoM joint surfaces. Thus, this paper will try to rationalize the available literature on in situ generated tribomaterial and propose reaction mechanisms that may explain their occurrence.

2 Clinical aspects

About 43% of failures registered in metal-on-metal (MoM) prostheses were attributed to adverse local tissue reactions (ALTRs). ALTRs, are the result of immune responses and clinically are shown as granulomas, necrotic tissue, pseudotumors, and systematic genotoxicity [16–17]. Although, the implantation prevalence of MoM has since 2008 declined from 40% to less than 3%, there are currently nearly one million patients carrying MoM bearings [18]. Clinically, the individual risk for each of these patients and the necessary management of these MoM bearings are not clearly understood [19].

Similarly to MoM bearings, modular junctions are also under scrutiny. Modular junctions have been introduced to handle complex deformity and keep hospital inventory low. They

also make joint reconstructions easier and faster for the surgeon. In a survey of the American Academy of Orthopaedic Surgeons among their members, 87% of the respondents indicated they have used implant modularity with a metal/metal taper junction [20]. On the flip side, modularity generates additional interfaces that can undergo fretting. Fretting is micro-motion caused by cyclic loading of modular junctions interfaces. Although this issue appeared to have been solved in the early 1990s, there are many new failure reports in the literature [21–23], and surgeons have to deal with the management of device failure due to ALTRs [24]. Certainly, a better understanding of the interaction of wear and corrosion, specifically factors which drive them towards protection and/or harmful degradation would help to establish management guidelines for those who carry devices with metal/metal interfaces in situ. (e.g. surface replacement devices which are still attractive for young athletic patients [25]).

Another clinical issue is the unknown composition of the degradation products, which are generated in the in vivo environment. Complex metal-protein compounds are generated [15]. Also, currently unknown, highly reactive products might be released from the contacting surfaces which decay to more stable debris products over time. Unfavourable reactions of these species with proteins and cells in the device vicinity may have stayed largely undetected because later histomorphological probing would show them in their equilibrium state. Hence, additional knowledge in this area would allow to design more relevant biocompatibility tests. Nowadays, the reaction of cells to corrosion products is assessed with diluted metal salts, or manufactured particles which are chemically stable [26].

In the following the paper will be focused on the degradation of MoM joint surfaces as one of the key factors determining clinical outcome of total hip joint replacements.

3 Wear and Metallurgical Transformations in MoM implants

In order to describe metallurgical transformation caused by friction and wear in metal-metal-contacts, one must look at the specific structure of any tribosystem characterized by the main tribo-elements (e.g. Head, Cup, Pseudosynovia, Human Body), the tribological loading (sliding, impact), ambient (37°C) and contact spot temperatures (up to approximately 60°C [27]) and the duration (as long as possible) [28]. These lead to a characteristic combination of acting wear mechanisms (adhesion, abrasion, surface fatigue, tribochemical reactions) and their submechanisms brought about by the dissipated work of friction [29]. Reported clinical linear wear rates for MoM hip replacements and joints under steady state conditions range from 1 to about 8 μm per year [30–31]. Assuming 0.5 to 3×10^6 gait cycles per year, the linear wear rate per gait cycle would be smaller than the size of an atom, while the size of the wear particles within the surrounding tissue starts at about 30 nm and ranges up to 10 μm [32–34], lying the majority of them in the nanometer size. This mismatch shows that such small wear rates, which are represented by the generation of wear particles and the release of ions, cannot be seen as a continuous process but should be understood as a highly localized and steadily altering sequence of void initiation, accumulation, and propagation on the nm-scale before any wear particles of such small size would detach from the surface.

3.1 Wear morphology

Well functioning MoM heads retrieved after 8 to 22 years typically exhibit organic reaction layers, indentations, remains of wear debris, and very few scratches (Figure 1). These are characteristic for “tribochemical reactions” and “surface fatigue” while there are very few indications (scratches) of “abrasion”. Even if abrasion would be apparent, the underlying submechanism could be microploughing, which generates grooves mainly by shifting the material towards the ridges instead of generating a chip like in microcutting [29]. Thus it is quite likely that under such small wear rates, microploughing prevails, bringing about a marked plastic deformation of the surface material. Still, because solid-solid contacts cannot be avoided in a self-mating metal contact under boundary and mixed lubrication conditions, adhesion could also be expected. However, there are no signs of “adhesion”, indicating that there is something hindering any direct metal-metal contacts. In addition, the reported nanometer-size wear particles are released from materials of much bigger grain sizes, ranging from 2 mm for cast prosthesis of the 1st generation to 30 μm of today’s cast and forged prostheses of 2nd and 3rd generation joints [36]. Thus the near-surface material must have undergone a marked microstructural alteration.

3.2 Strain Gradient from Bulk to Surface

MoM bearings, as it is for any other tribosystem, show a distinct run-in followed by steady-state [37]. Thus, in the beginning, both contacting surfaces undergo a process of adjustment by either wear and/or plastic deformation before the contacting bodies interact predominantly elastic [31, 38–40]. Importantly, at such small wear rates, the elastic interaction is of cyclic nature during steady-state and, therefore, might allow for cyclic-plastic deformation (cyclic-creep or ratcheting) [41–43] followed by mechanical instabilities like shear bands [44–48] as well as crack initiation and propagation [49–51]. Finally the microstructure of standardized HC-CoCrMo alloys might vary markedly depending on the production route and sequence [52], with still unknown relations to the actual wear or corrosion behavior.

3.2.1 Bulk and Sub-Surface Strain Gradient—The strain gradient is displayed along the increasing contact stresses, as computed according to Hamilton et al. [53] and Fischer et al. [54], and starts from the nominally stress-free bulk. Close to the surface, the so-called “sub-surface” volume undergoes multiaxial fatigue stress due to the cyclic nature of friction. This leads to the accumulation of plastic strain forming a ratchetting gradient. For CoCrMo-alloys this mechanism is brought about solely by planar slip generating the triangle and rhomboid areas (Figure 2), which – by the increasing stress amplitudes towards the surface – become smaller [44, 55].

3.2.2 Near-Surface Strain Gradient and Tribomaterial—Directly at and underneath the contacting surface – within the “near-surface” volume – signs of severe plastic deformation are found accompanied by so-called mechanical instabilities like shear bands. Such instabilities do either generate from the accumulated cyclic shear [43, 57] or are generated monotonically by severe plastic deformation [49, 58], while on the basis of recent experimental and computational findings, the latter appears more likely [59, 60]. The grain size remains between 10 to 70 nm at depths from 100 to 300 nm (Figure 3). The motion

between head and cup is accommodated by this thin layer of nanostructured material, since it can undergo the high shear rates of 10^3 to 10^5 s^{-1}. As proposed earlier, molecular dynamic simulations have shown a friction-induced rotation of randomly arranged clusters of atoms or a spontaneous generation of rotating nanocrystals on the interface of solid sliding bodies in contact [61]. This mechanism will bring about a zone of rotating matter, which is also known for severe plastic deformation of nanocrystalline metals under shear [62]. Any interfacial medium like the pseudosynovia is now incorporated into such nanometer-size vortices and a nanostructured composite consisting of the lubricant and the severely strained materials of body and counterbody is generated (Figure 3) [9].

Thus this uppermost layer, sometimes referred to as third-body material [63], alters its chemical composition by mechanical mixing [64], a submechanism of tribochemical reactions.

Recently, fine machining experiments [61] and computer simulations [59, 65] have shown that, for microcrystalline materials, such rotation occurs mainly by microploughing during run-in. Grain boundaries act as obstacles for shear and lead to overfolding. MoM laboratory experiments also support these findings, that most of the tribomaterial is generated during run-in [66]. During steady state this nanostructured composite layer is worn by surface fatigue brought about either by blunt asperities (delamination), or by rotating nanosize wear debris (indentation), or it reaches its critical thickness and spalls off as it is known for tribochemical reactions. The growth rate of tribomaterial can in part balance the weight loss by surface fatigue and, therefore, allow for such very small wear rates of some nm/h.

4 Chemical and electro-chemical behaviour of CoCrMo in body fluids

Corrosion of CoCrMo alloys exposed to synovial fluid encompasses a variety of chemical surface transformations arising from chemical and electrochemical reactions of the metal and the liquid environment. As in the case of most alloys, the corrosion behaviour of CoCrMo alloys is highly dependent on chemical composition, microstructure (phases, inclusions and defects) and surface state. Synovial fluid is a viscous, non-Newtonian aqueous solution containing inorganic salt constituents (i.e. chlorides, phosphates, carbonates), organic molecules (proteins [e.g. albumin, globulin], glycoproteins [e.g. lubricin], glycosamins [e.g. hyaluronic acid], lipids, proteinases, and collagenases among others) and cells [67]. This corrosion system is clearly complex and, not surprisingly, still only partially understood.

4.1 Electrochemical reactions of CoCrMo alloys

CoCrMo surfaces can experience four different corrosion conditions: immunity, active metal dissolution, passivity and transpassive metal dissolution. Passivity is the most common situation under the operating conditions of the alloy in the human body (analysis of retrievals showed there is an oxide film on the explants [68]). It is defined as the electrochemical situation where the formation of a 2–10 nm thin oxide film takes place. The latter is essentially composed of Cr_2O_3 [69], since Co usually actively dissolves in body fluids. Such oxide film reduces the dissolution rate of the metal by acting as a physical barrier limiting the transport of electrons, cations and anions between the metal and the

electrolyte and reducing the kinetics of the anodic and cathodic reactions underlying the corrosion process. The thickness of the passive film on CoCrMo alloys and its composition changes with potential [69–71]. Typically, above 0 V_{SHE} (SHE: standard hydrogen electrode) the film thickness rapidly increases with potential at a rate of approximately 10nm/V [61]. Under heavily oxidizing conditions, the trivalent chromium oxide, the main constituent of passive films on CoCrMo alloys, may become unstable and dissolve in form of soluble Cr^{6+} [69–71]. The passivity is lost and the metal is in the so-called transpassive state.

The electrode potential defines the corrosion conditions of the metal as indicated in Figure 4. The graph is based on thermodynamic data of the main constituents of CoCrMo alloy [72].

The electrode potential spontaneously reached by a metal in an electrolyte (the so-called ‘open circuit potential’ or OCP) is a non-equilibrium potential that depends on the kinetics of both the metal oxidation and the reduction of the oxidant. The electrode potential is difficult to predict and requires experimental determination for each specific corrosion system. Recently, open circuit potentials of a low-carbon CoCrMo alloy measured in-vivo in synovial fluids extracted from a cohort of patients have been reported between 0.1 to 0.3 V_{SHE} [73] with most patients exhibiting a potential very close to 0.15 V_{SHE}. Thus, CoCrMo implants are expected to undergo active dissolution of Co, transpassive dissolution of Mo and passivation by Cr. It should be noted, however, that transpassive conditions can be reached also for Cr in case of high potentials. Corrosion rates varying from 50 to 750 mg dm^{-2} i.e. linear corrosion rates from 0.6 to 10 μm/year, were reported by Igual Munoz et al. [73]. These corrosion rates may impact periprosthetic tissue contamination by metal ions since they are in the same range as those reported for in-vivo wear rates (see section 3).

4.2 Electrochemical reactions of the environment

Typical oxidizing species in body fluids or simulated body fluids are dissolved oxygen and water. However, there are also intermediate oxygen species (i.e. free radicals, peroxides) in those reduction reactions that can dramatically modify the behaviour of the metal in the synovial fluid. These intermediates may also have effects on the biological system, like for example inducing oxidative stress in cells [74]. Corrosion itself can stimulate reactive oxygen species (ROS) production as intermediate products and trigger further oxidative response from cells [75]. Cells are known to produce ROS such as hydrogen peroxide [75] as a consequence of inflammation or mechanical stress. Protein-like molecules can also act as oxidizer through the reduction of their disulphide bonds [76]. The ionic salts in principle do not directly participate in reduction reactions but can weaken passive films and thus promote metal oxidation [77]. The nature and properties of the oxidant determines the electrode potential thus affecting the surface chemistry and electrochemical response of the alloy.

4.3 Adsorption of organic molecules

The presence of adsorbed species at the metal-liquid interface may influence electrochemical processes involved in corrosion in many ways. By binding metal ions (*organometallic complexes formation*) and transporting them away from the solution/

biomaterial interface, organic molecules such as proteins can enhance corrosion [71]. Albumin adsorbed on CoCrMo alloys inhibits oxygen reduction [78] while at the same time increases passive film dissolution [79]. Protein surface interactions with Molybdenum ions have been reported as crucial factors affecting the transpassive behaviour of CoCrMo alloys [80, 81]. Protein adsorption is a complex process in which the prevailing electrochemical conditions, the structure of proteins, the ionic strength and the pH of the solution, and metal surface properties influence the affinity of the protein for a given interface [82]. Albumin adsorption, for example, is known to be dependent on the potential of the metal [79]. Although the reactivity of organic molecules in contacts can hardly be predicted at present, it can play a relevant role in the overall corrosion and wear process. Further experimental investigations coupled with Molecular Dynamic simulations may shed in future additional light on these reactions.

4.4 Tribocorrosion

Finally, electrochemical behaviour is crucial in the presence of tribological and/or mechanical stress, such as sliding wear, fretting wear, and fatigue loading. Recently, based on a meta analysis of published CoCrMo wear studies [6], it has been shown that the variability of CoCrMo wear in various electrolytes and tribocontacts can be explained by using the electrode potential as key factor. Wear rates were found to undergo a transition from low to high wear rates at approximately 0 V_{SHE} [6]. This potential corresponds approximately to the threshold for the onset of passive film thickening [69] as discussed in 4.1. This is a clear indication that wear-accelerated corrosion due to repeated depassivation and repassivation of worn areas contributes significantly, together with mechanical removal of metal particles, to the overall degradation of CoCrMo alloys in aqueous solutions. In a tribocorrosion contact the mechanically-induced depassivation of the worn areas typically shifts the electrode potential towards lower values through a galvanic coupling mechanism [83]. For example, Yu Yan and colleagues measured a drop of up to 0.3 V during the motion in a hip joint simulator [84], compared to the overall potential under static conditions. Note that locally, in particular in depassivated areas, the electrode potential can drop much more during rubbing [83]. The mechanically-induced potential decay can be described through tribo-electrochemical models [83] by taking the kinetics of the cathodic reaction and the ratio of the depassivated (worn) and still passive (unworn) areas into account. The model has been successfully applied to different alloys and conditions [85].

5 Tribomaterial in Metal/Metal implant contacts

Several studies in the literature have reported about the formation of tribomaterial in MoM hip joints tested in-vivo and in-vitro. Table 1 summarizes published results, in chronological order, on surface transformation occurring on CoCrMo alloys.

In-vitro studies [86, 87, 89, 94, 48] consistently report the build-up of carbonaceous layers while in-vivo results mention a variety of surface films ranging from thick oxide films to organic or even graphitic layers [9, 92]. This is not surprising since in-vitro studies are executed in a well-defined environment (e.g. calf serum) while the nature of the in-vivo environment is subject to variability and patient-specific. This has been confirmed by a

recent investigation showing significant differences in the electrochemical behaviour of a LC-CoCrMo alloy in synovial fluids extracted from different patients [73]. The most detailed chemical analysis of the layer was carried out by Wimmer et al. [9] using XPS, a technique that combines high depth resolution (1 nm) and the possibility to obtain quantitative information on the elements and their chemical states. In this study, a thick oxide film containing organic matter and salts was identified. Other studies [86–89, 94] made use of EDS analysis, which is efficient in detecting elements, but it suffers of shortcomings in the quantification of light elements such as C and O. Indeed, no author provided any atomic composition of the layer. However, their qualitative results are all consistent with the XPS analysis published by Wimmer et al. [9]. In one case, EELS was used to identify the presence of the graphitic layer [92].

TEM is the preferred technique for characterizing metallurgical transformation of the surfaces. The build-up of a near surface nano-crystalline layer and strain accumulation in the metal underneath has been generally observed in-vivo and in vitro. TEM results reach a certain consensus on the thickness (30–200 nm) and structure (grain size between 15–40 nm) of this nano-cystalline layer [52, 9, 86–88, 90–93]. Note, however, that one of these studies reported that the nano-crystalline layer could be only observed locally on retrieved implant surfaces [93]. Obviously the loading history of any specific small spot within the contact area that is analysed by high-resolution techniques must be known. The extreme localization of tribological events at small wear rates [66, 95, 96] renders different appearances within very small geometrical scales.

The effect of pressure on wear particle characteristics has been investigated in-vitro by Pourzal et al. [91] using TEM coupled with EDS for chemical characterization. The authors reported that the nature and size of the particles depend on the contact pressure and on kinematics. The particles generated in heavily loaded (135 MPa contact pressure) reciprocating motion contacts [91] were found to be one order of magnitude larger than the 30–80 nm wear particles found in simulators (30 MPa contact pressure) [91]. The particles can be metallic, partially or completely oxidised. The latter appeared to be generated by flaking of larger debris. It should be mentioned here that other groups mostly found oxidized wear particles from in-vitro and in-vivo analyses [32–34, 97–99]. Thus the knowledge about the generation sequence as well as the reaction kinetics still remains fragmentary.

6 Discussion

6.1 Origin of the surface reaction film

Analysing the published results on surface composition of MoM CoCrMo bearing surfaces, one can identify three cases with specific features of the tribofilm (Figure 5). The first case is characterised by the presence of thick oxide layers (up to 100 nm on the metal surface). The second case involves the formation of relatively thick organic matter directly on the oxide-free metal surface. The third situation is characterized by the formation of a relatively thin oxide layer (5–10 nm) formed on the metal surface and covered by an organic layer of approximately 50 nm thickness. The organic layers are attributed to protein decomposition caused by the high contact pressure and temperature between contact spots [9]. In the

following the origin of these features will be discussed based on the current knowledge in metallurgy, corrosion and wear of this alloy system.

Case 1: oxide surface reaction layer—Wimmer et al. [9] analysed 42 retrieved McKee-Farrar hip prosthesis, over 80% of the heads and cups presented layers of varying thicknesses on the articulating surfaces. XPS depth profiles were carried out by these authors on the non-contacting and the contacting areas. On the non-contacting areas one can see a typical passive surface structure consisting of an external carbon contamination layer and an oxide film (passive film) covering the metal substrate. The layer composition and thickness (5–10 nm) correspond well with already reported results of passive films on CoCrMo in simulated body fluids [69, 70, 80]. The articulating surface showed a very different surface composition. The same carbon contamination was present but the oxide film was thicker (ca 100 nm) and contains carbon, nitrogen, phosphorous, calcium and chromium. At half thickness, the composition of the oxide film as extracted from the depth profiles was 55 at.% O, 3 at.% of N, 9 at.% of Ca, 7 at.% of P, 8 at.% of C and 19 at.% Cr. The oxidation state of the elements was determined from the XPS peak position: N was related to organic compounds, Cr and Ca were related to an oxidized state, and phosphorous to phosphates. The C signal presented characteristic peaks of typical bond found in organics such as C-C, C-H, C-O and C-N. Therefore, this composition most likely corresponded to a mixture of organic compounds as well as calcium phosphate and chromium oxide.

The build up of such a thick passive film is not compatible with classical metal oxidation mechanisms, involving high field conduction or diffusion of ions through the growing oxide film. First, high field conduction requires electrical fields across the oxide film of typically 1 V/nm i.e. unrealistic implant electrode potential of 100 V. Solid state diffusion at the low temperature characterizing the human body is too slow to enable the formation of thick oxide film: for comparison oxidation of a CoCrMo alloy at 300 ºC over several days yielded oxide film thicknesses of 30 nm only [100]. Instead, other mechanisms such as cracking of the oxide film under the frictional stress field followed by oxide regrowth at crack tips and, depending on shear stress amplitude, mechanical mixing with species such as phosphates, calcium and organic molecules adsorbing or depositing on the oxide surface may take place. Note that from the electrochemical point of view, this mechanism implies electrode potentials of the rubbing surfaces above the passive potential of the metal (−0.8 V_{SHE} for chromium).

Another mechanism, based on the third body approach [63], consists in the following sequence: detachment of metal particles followed by their oxidation while suspended in water, adsorption of organic species on the particles, particle agglomeration and sedimentation, as well as possible compaction during tribological contact. If this mechanism was acting, one would expect to find partially oxidized metallic particles in the tribofilm. This was however not confirmed by the XPS analysis [9] that could not detect alloy elements in their metallic state within the tribofilm.

Possibly, a combination of both mechanisms takes place. The relative influence of each mechanism depends on the prevailing chemical and mechanical conditions.

Case 2: organic surface reaction layer—A pure organic film was found [90] on a sample from the same set of retrievals analysed in the previous case [9]. The chemical composition of the organic layer consists of C, O and N and results from deposition of proteins. The absence of a passive film at the interface between the organic tribofilm and the bulk metal was noticeable and from the electrochemical point of view, this indicates that the electrode potential of the concerned metal surface lies below the passivation potential (−0.8 V_{SHE} for chromium). Recent results by Igual et al [78] showed that albumin deposition is activated by the production of hydrogen through cathodic water reduction occurring at potentials below −0.8 V_{SHE}. This activation leads to a steady growth of the deposit protein layer up to thicknesses above five monolayers at the rate of 3 nm/minute. However, on the other hand, deposition of albumin at passive potentials (above −0.8 V_{SHE} for chromium) leads only to a maximum of one monolayer coverage [79].

Those low cathodic potentials can be reached in implants when tribocorrosion contacts cause a galvanic coupling between the passive areas and the mechanically depassivated zones. Several authors have reported cathodic potential values while rubbing in different passive materials such as CoCrMo, Stainless steels or Titanium alloys [83, 85]. For example, Vieira et al. [83] estimated a cathodic potential as low as −1.5 V_{SHE} in the contact area of an aluminium alloy rubbing against an alumina ball in NaCl.

Case 3: bilayer surface reaction layer—This situation was encountered in a MoM hip joint tested in a simulator [84]. It consists in an inner oxide film of 5–10 nm covered by an outer Carbon-rich layer of thickness of 15–20 nm. This feature is consistent with an alloy in its passive state and covered by organic molecules. Such situation was throughout investigated by Valero et al. [79], who found that adsorption of albumin increases with the applied passive potential with a maximum coverage of one monolayer for a protein concentration of 0.5 g/L. However fluid protein concentration is larger in the body and therefore thicker organic deposits are expected. In the transpassive potential, protein adsorption on an oxide film was also observed [79]. At this transpassive potential, the dissolution of Mo(VI) ions may additionally promote protein deposition [81]. Although the bilayer tribofilm is compatible with both a passive and transpassive state of the alloy, transpassive potentials require the presence of strong oxidising agents. Those oxidising agents can be present in the synovial fluid due to inflammatory cell processes in the surrounding tissues [101] or can be in principle be generated locally at contact spots undergoing high temperatures. In the former case, based on mechanisms proposed by Martin et al. [81], one would expect a reaction film that covers the whole surface, while in the latter case, the tribofilm would form in the localized contact zone only.

6.2 Wear mechanisms

The work of Pourzal et al. [90, 91] on wear particles clearly points out to the relevance of subsurface transformations including the formation of nano-crystalline layers and ε-martensite. Indeed, the nature of the particles was intimately related to the one of the transformed near-surface zone. This zone is schematically described in Figure 6, where the near-surface zone is divided in an outermost nano-crystalline layer and a subjacent highly strained layer containing twins and ε-martensite [93].

At low contact pressures (i.e. few tens of MPa) wear debris is generated either by detachment of single grains from the nano-crystalline layer (nano-wear mechanism [3]), or by cracking within the nano-crystalline layer (release of clusters of nano-grains). As the contact pressure becomes larger, the stress field reaches deeper into the subsurface causing failure within the strained layer. This leads to the release of larger wear particles. The model matches the findings of Pourzal et al. [91] who found at high loads (non-conformal tribometer contact) larger wear particles (30–80 nm) with martensitic structure, while at lower loads (conformal hip joint simulator contact) there were only smaller particles (5–15 nm).

Clearly, the locally supported load plays a crucial role in determining the wear mechanisms. In a sense the presence of surface reaction layers lowers the stress field acting on the near-surface zone of the metal by bearing part of the load. This would favour the emission of smaller wear particles and thus a less severe wear mechanism, so-called ultra-mild wear. Therefore, the generation of this surface reaction layer would constitute a way to minimize wear of MoM hip implants. On the other hand, the influence of this surface reaction layer on the corrosion response of the formed material is still unknown because of the scarce number of publications dedicated to this issue. Indeed, only two authors [56, 103] have studied the effect of the tribofilm on the electrochemical behaviour of implants and still no clear conclusions can be drawn. However, as a prerequisite for the intentional use of tribofilms in hip bearings, a better understanding of the conditions under which such layers form is needed. In particular, this work highlights that the electrochemical conditions are a determining factor in controlling the nature of surface reactions. Since the electrochemical response of the implant is dependent on synovial fluid chemistry as well as on the local mechanical conditions, a better understanding about their influence on metallic implant material degradation is needed.

7 Conclusions

The analysis of existing literature in metallic implant material degradation performed in this paper has revealed the following:

- Several analytical techniques have been utilized in studies that reported surface transformations in MoM contacts. These studies provided detailed pictures of chemical, mechanical and/or metallurgical phenomena. However, these observations were never applied in combination and therefore available results in literature give only fragmented information.

- Based on the information found in the literature, three distinct tribomaterial structures can be described: metal surface covered by thick oxide film, metal surface covered by organic layer without intermediate oxide film, and finally metal surface covered by a thin oxide film with a superimposed organic layer. The near surface zone of the metal typically presents a nanocrystalline structure.

- By taking the prevailing loading and the electrochemical conditions in the contact into account, mechanisms leading to tribomaterial formation and wear particle generation can be rationalised.

As a general conclusion, this study has shown that the existing theoretical concepts can be successfully applied to gain better insight into the behavior of MoM wear. In future work, these concepts need to be validated by dedicated in-vivo or in-vitro experiments conducted under well-defined electrochemical and mechanical conditions, accompanied by a comprehensive chemical and metallurgical pre- and post-wear characterization of the samples.

Acknowledgments

Alfons Fischer and Markus Wimmer received support from the National Institutes of Health (NIH RC2AR058993)

References

1. Katz JN, Winter AR, Hawker G. Measures of the Appropriateness of Elective Orthopaedic Joint and Spine Procedures. J Bone Joint Surg Am. 2017 Feb 15.99(4):e15.doi: 10.2106/JBJS.16.00473 [PubMed: 28196043]
2. Kurtz SM, Ong KL, Lau E, Bozic KJ. Impact of the economic downturn on total joint replacement demand in the United States: updated projections to 2021. J Bone Joint Surg Am. 2014; 96:624–30. [PubMed: 24740658]
3. Landolt, D., Mischler, S. Tribocorrosion of Passive Metals and Coatings. Woodhead Publishing; Lausanne: 2011.
4. Mathew MT, Jacobs JJ, Wimmer MA. Wear-Corrosion Synergism in a CoCrMo Hip Bearing Alloy is Influenced by Proteins. Clin Orthop. 2012; 470:3109–3117. [PubMed: 22956237]
5. Neville, Mathew book chapter 12, 13Mathew MT, Srinivasa Pai P, Pourzal R, Fischer A, Wimmer MA. Significance of tribocorrosion in biomedical applications: overview and current status. Advances in Tribology. 2009; 2009:1–12.
6. Mischler S, Igual Munoz A. Wear of CoCrMo alloys used in metal-on-metal hip joints: A tribocorrosion appraisal. Wear. 2013; 297:1081–1094.
7. Cao S, Guadalupe Maldonado S, Mischler S. Tribocorrosion of passive metals in the mixed lubrication regime: theoretical model and application to metal-on-metal artificial hip joints. Wear. 2015; 324–325:55–63.
8. Cao S, Mischler S. Assessment of a recent tribocorrosion model for wear of metal-on-metal hip joints: Comparison between model predictions and simulator results. Wear. 2016; 362–363:170–178.
9. Wimmer MA, Sprecher C, Hauert R, Tager G, Fischer A. Tribochemical reaction on metal-on-metal hip joint bearings: A comparison between in-vitro and in-vivo results. Wear. 2003; 255(7–12):1007–1014.
10. Myant C, Cann P. On the matter of synovial fluid lubrication: Implications for metal-on-metal hip tribology. J Mech Behav Biomed. 2014; 34:338–348.
11. Langton DJ, Jameson SS, Joyce TJ, Hallab NJ, Natu S, Nargol AV. Early failure of metal-on-metal bearings in hip resurfacing and large-diameter total hip replacement: A consequence of excess wear. J Bone Joint Surg Br. 2010 Jan; 92(1):38–46. [PubMed: 20044676]
12. MHRA (Medicines and healthcare products regulatory agency) Medical Device Alert Ref.: MDA/2012/036 (2012). FDA (US Food and Drug Administration) Metal-on-metal Hip Implant Systems. FDA Executive Summary Memorandum, Othopaedic and Rehabilitation Devices Advisory Panel Gaithersburg; Maryland: 2012.
13. Australian Orthopaedic Association. Annual Report. Adelaide: AOA; 2015. National Joint Replacement Registry.
14. Jacobs JJ, Gilbert JL, Urban RM. Current Concepts Review-Corrosion of Metal Orthopaedic Implants. The Journal of Bone and Joint Surgery (American). 1998; 80:268–82.
15. Milosev I, Remskar M. In vivo production of nanosized metal wear debris formed by tribochemical reaction as confirmed by high-resolution TEM and XPS analyses. J Biomed Mater Res A. 2009; 91:1100–1110. [PubMed: 19107790]

16. Willert H-G, Buchhorn GH, Dipl-Ing Fayyazi A, Flury R, Windler M, Köster G, Lohmann CH. Metal-on-Metal Bearings and Hypersensitivity in Patients with Artificial Hip JointsA Clinical and Histomorphological Study. J Bone Jt Surg Am. 2005; 87:28–36.
17. Dunstan E, Ladon D, Whittingham-Jones P, Carrington R, Briggs TWR. Chromosomal aberrations in the peripheral blood of patients with metal-on-metal hip bearings. J Bone Joint Surg Am. 2008; 90:517–522. [PubMed: 18310701]
18. Kurtz, SM., Ong, KL., Lau, E., Greenwald, AS., Bozic, K. Met.–Met Total Hip Replace Devices. Kurtz, SM.Greenwald, AS.Mihalko, WM., Lemons, JE., editors. ASTM International; 2013. p. 3-18.
19. Hannemann F, Hartmann A, Schmitt J, Lützner J, Seidler A, Campbell P, Delaunay CP, Drexler H, Ettema HB, García-Cimbrelo E, Huberti H, Knahr K, Kunze J, Langton DJ, Lauer W, Learmonth I, Lohmann CH, Morlock M, Wimmer MA, Zagra L, Günther KP. European multidisciplinary consensus statement on the use and monitoring of metal-on-metal bearings for total hip replacement and hip resurfacing. Orthop Traumatol Surg Res OTSR. 2013; 99:263–271. [PubMed: 23507457]
20. Mihalko WM. Survey results concerning modular taper junctions among fellows of the American Academy of Orthopaedic Surgeons. ASTM Work Modul Tapers Total Jt Replace Devices Jacksonv FL. 2013
21. Lindgren JU, Brismar BH, Wikstrom AC. Adverse reaction to metal release from a modular metal-on-polyethylene hip prosthesis. J Bone Joint Surg Br. 2011; 93:1427–1430. [PubMed: 21969447]
22. Gill IPS, Webb J, Sloan K, Beaver RJ. Corrosion at the neck-stem junction as a cause of metal ion release and pseudotumour formation. J Bone Joint Surg Br. 2012; 94:895–900. [PubMed: 22733942]
23. Cooper HJ, Urban RM, Wixson RI, Meneghini RM, Jacobs JJ. Adverse Local Tissue Reactions Arising from Corrosion at the Neck-Body Junction in a Dual Taper Stem with a CoCr Modular Neck. J Bone Joint Surg Am. 2013; 95:865–872. [PubMed: 23677352]
24. Plummer DR, Berger RA, Paprosky WG, Sporer SM, Jacobs JJ, Della Valle CJ. Diagnosis and Management of Adverse Local Tissue Reactions Secondary to Corrosion at the Head-Neck Junction in Patients With Metal on Polyethylene Bearings. Journal of Arthroplasty. 2016; 31:264–268.
25. Kamath AF, Prieto H, Lewallen DG. Alternative bearings in total hip arthroplasty in the young patient. Orthop Clin North Am. 2013 Oct; 44(4):451–62. [PubMed: 24095062]
26. Catelas I, Wimmer MA, Utzschneider S. Polyethylene and metal wear particles: characteristics and biological effects. Semin Immunopathol. 2011; 33:257–271. [PubMed: 21267569]
27. Wimmer MA, Loos J, Nassutt R, Heitkemper M, Fischer A. The Acting Wear Mechanisms on Metal-on-Metal Hip Joint Bearings – in vitro Results. Wear. 2001; 250:129–139.
28. Czichos H, Dowson D. Tribology: A systems approach to the Science and Technology of friction, lubrication and wear. Tribology International. 1978; 11:259–260.
29. Zum Gahr, KH. Microstructure and Wear of Materials. Elsevier Science Publishers; Amsterdam, The Netherlands: 1987.
30. Unsworth A, Scholes SC, Smith SL, Elfick APD, Ash HA. Tribology of replacement hip joints. Tribology Series. 2000; 38:195–202.
31. Firkins PJ, Tipper JL, Saadatzadeh MR, Ingham E, Stone MH, Farrar R, Fisher J. Quantitative analysis of wear and wear debris from metal-on-metal hip prostheses tested in a physiological hip joint simulator. Biomed Mater Eng. 2001; 11:143–157. [PubMed: 11352113]
32. Doorn PF, Campbell PA, Worrall J, Benya PD, McKellop HA, Amstutz HC. Metal wear particle characterization from metal on metal total hip replacements: transmission electron microscopy study of periprosthetic tissues and isolated particles. J Biomed Mater Res. 1998; 42:103–111. [PubMed: 9740012]
33. Catelas I, Bobyn JD, Medley JB, Krygier JJ, Zukor DJ, Huk OL. Size, shape, and composition of wear particles from metal-metal hip simulator testing: effects of alloy and number of loading cycles. J Biomed Mater Res A. 2003; 67:312–327. [PubMed: 14517891]
34. Billi F, Benya P, Ebramzadeh E, Campbell P, Chan F, McKellop HA. Metal wear particles: What we know, what we do not know, and why. SAS Journal. 2009; 3:133–142. [PubMed: 25802639]

35. Sprecher, Christoph. Beschreibung der Ablagerungen auf Metall-Metall-Paarungen an Hüftendoprothesen, Diplomarbeit. Interstaatliche Hochschule für Technik Buchs NTB; Buchs (Switzerland): 2002.
36. Büscher, R. PhD-Thesis University of Duisburg-Essen, 2005. VDI Verlag; Düsseldorf, Germany: 2005. Gefügeumwandlung und Partikelbildung in künstlichen Metall/Metall-Hüftgelenken. Fortschr.-Ber. VDI-Z, Reihe 17: Biotechnik/Medizintechnik, Nr. 256
37. Silva M, Heisel C, Schmalzried TP. Metal-on-metal total hip replacement. Clinical Orthopaedics and Related Research. 2005:53–61. [PubMed: 15662304]
38. Walker PS, Gold BL. The tribology (friction, lubrication and wear) of all-metal artificial hip joints. Wear. 1971; 17:285–299.
39. Plitz W, Huber J, Refior HJ. Experimental studies of metal-metal slide combinations and their value in relation to expected in-vivo behavior. Orthopäde. 1997; 26:135–141. [PubMed: 9157353]
40. Silva M, Schmalzried TP. Metal-on-metal: History, basic science, and toxicity. Seminars in Arthroplasty. 2003; 14:113–122.
41. Dupont F, Finnie I. The simulation of sliding wear by cyclic deformation: Microstructural aspects. Wear. 1990; 140:93–106.
42. Su X, Clayton P. Ratchetting strain experiments with a pearlitic steel under rolling/sliding contact. Wear. 1997; 205:137–143.
43. Fischer A, Weiss S, Wimmer MA. The tribological difference between biomedical steels and CoCrMo-alloys. Journal of the Mechanical Behavior of Biomedical Materials. 2012; 1:50–62.
44. Rainforth WM, Stevens R, Nutting J. Deformation structures induced by sliding contact. Philos Mag A. 1992; 66:621–641.
45. Biswas SK. Wear of metals: A consequence of stable/unstable material response. Proceedings of the Institution of Mechanical Engineers, Part J: Journal of Engineering Tribology. 2002; 216:357–369.
46. Tarasov SY, Kolubaev AV. Generation of shear bands in subsurface layers of metals in sliding. Physics of the Solid State. 2008; 50:844–847.
47. Kolubaev A, Tarasov S, Sizova O, Kolubaev E. Scale-dependent subsurface deformation of metallic materials in sliding. Tribology International. 2010; 43:695–699.
48. Zeng P, Rana A, Thompson R, Rainforth WM. Subsurface characterisation of wear on mechanically polished and electro-polished biomedical grade CoCrMo. Wear. 2015; 332–333:650–661.
49. Jahanmir S, Suh NP, Abrahamson EP II. The delamination theory of wear and the wear of a composite surface. Wear. 1975; 32:33–49.
50. Jahanmir S, Suh NP. Mechanics of subsurface void nucleation in delamination wear. Wear. 1977; 44:17–38.
51. Fleming JR, Suh NP. Mechanics of crack propagation in delamination wear. Wear. 1977; 44:39–56.
52. Stemmer, P., Pourzal, R., Liao, Y., Marks, L., Morlock, M., Jacobs, JJ., Wimmer, MA., Fischer, A. Microstructure of retrievals made from standard cast HC-CoCrMo alloys. In: Kurtz, SM.Greenwald, AS.Mihalko, WM., Clemson, JE., editors. ASTM STP 1560 Metal-on-Metal Total Hip Replacement Devices. ASTM; West Conshohocken PA, USA: 2013. p. 251-267.
53. Hamilton GM. Explicit equations for the stresses beneath a sliding spherical contact, Proceedings of the Institution of Mechanical Engineers, Part C. Mechanical Engineering Science. 1983; 197:53–59.
54. Fischer A. Subsurface Microstructural Alterations during Sliding Wear of Biomedical Metals. Modelling and Experimental Results. Computational Materials Science. 2009; 46:586–590.
55. Büscher R, Fischer A. The pathways of dynamic recrystallization in all-metal hip joints. Wear. 2005:887–897.
56. Pourzal, R. PhD-Thesis University Duisburg-Essen. Duisburg, Germany: VDI Verlag; 2011. Possible Pathways of Particle Formation in CoCrMo Sliding Wear. Fortschr Ber VDI Z, 17(285)Düsseldorf, Germany
57. Huang JY, Wu YK, Ye HQ. Microstructure investigations of ball milled materials. Microsc Res Tech. 1998; 40:101–121. [PubMed: 9504123]

58. Zhu R, Zhou J, Jiang H, Zhang D. Evolution of shear banding in fully dense nanocrystalline Ni sheet. Mechanics of Materials. 2012; 51:29–42.
59. Beckmann N, Romero PA, Linsler D, Dienwiebel M, Stolz U, Moseler M, Gumbsch P. Origins of Folding Instabilities on Polycrystalline Metal Surfaces. Physical Review Applied. 2014; 2:064004.
60. Sundaram NK, Guo Y, Chandrasekar S. Mesoscale folding, instability, and disruption of laminar flow in metal surfaces. Physical Review Letters. 2012; 109
61. Rigney DA, Karthikeyan S. The evolution of tribomaterial during sliding: A brief introduction. Tribology Letters. 2010; 39:3–7.
62. Valiev R. Nanostructuring of metals by severe plastic deformation for advanced properties. Nature Materials. 2004; 3:511–516. [PubMed: 15286754]
63. Godet M. The third-body approach: A mechanical view of wear. Wear. 1984; 100:437–452.
64. Karthikeyan S, Agrawal A, Rigney DA. Molecular dynamics simulations of sliding in an Fe-Cu tribopair system. Wear. 2009; 267:1166–1176.
65. de Beer S, Müser MH. Viewpoint – Surface Folds Make Tears and Chips. Physics. 2012; 5
66. Fischer A, Stickel D, Schoss C, Bosman R, Wimmer MA. On the Growth Rate of Tribomaterial in Bovine Serum Lubricated Sliding Contacts. Lubricants. 2016; 4:21.doi: 10.3390/lubricants4020021
67. Tamer TM. Hyaluronan and synovial joint: function, distribution and healing. Interdisciplinary Toxicology. 2013; 6:111–125. [PubMed: 24678248]
68. Gkagkalis G, Mettraux P, Omoumi P, Mischler S, Rüdiger HA. Adverse tissue reaction to corrosion at the neck-stem junction after modular primary total hip arthroplasty. Orthopaedics & Traumatology: Surgery & Research. 2015; 101:123–126.
69. Hodgson AWE, Kurz S, Virtanen S, Fervel V, Olsson COA, Mischler S. Passive and transpassive behaviour of CoCrMo in simulated biological solutions. Electrochimica Acta. 2004; 49:2167–2178.
70. Milošev I, Strehblow H-H. The composition of the surface passive film formed on CoCrMo alloy in simulated physiological solution. Electrochimica Acta. 2003; 48:2767–2774.
71. Igual Munoz A, Mischler S. Interactive effects of albumin and phosphate ions on the corrosion of a CoCrMo implant alloy. Journal of The Electrochemical Society. 2007; 154:C562–C570.
72. Pourbaix M. Atlas of electrochemical equilibria in aqueous solutions. NACE Inter. 1974
73. Igual Munoz A, Schwiesau J, Jolles BM, Mischler S. In vivo electrochemical corrosion study of a CoCrMo biomedical alloy in human synovial fluids. Acta Biomaterialia. 2015; 21:228–236. [PubMed: 25797841]
74. Gilbert JL, Sivan S, Yangping Liu, Kocagöz S, Arnholt C, Kurtz SM. Evidence of direct cell induced corrosion of CoCrMo implant systems, Abstract #452. Soc Biomater. 2014
75. Kalbacova M, Roessler S, Hempel U, Tsaryk R, Peters K, Scharnweber D, et al. The effect of electrochemically simulated titanium cathodic corrosion products on ROS production and metabolic activity of osteoblasts and monocytes/macrophages. Biomaterials. 2007; 28:3263–72. [PubMed: 17466367]
76. Stankovich MT, Bard AJ. The electrochemistry of proteins and related substances part III. Bovine Serum Albumin. J Electroanal Chem. 1978; 86:189–199.
77. Olsson C-OA, Landolt D. Passive films on stainless steels – structure and growth. Electrochimica Acta. 2003; 48:1093–1104.
78. Igual Munoz A, Mischler S. Electrochemical Quartz Crystal Microbalance and X-Ray Photoelectron Spectroscopy study of cathodic reactions in Bovine Serum Albumin containing solutions on a Physical Vapour Deposition-CoCrMo biomedical alloy. Electrochimica Acta. 2015; 180:96–103.
79. ValeroVidal C, Igual Muñoz A, Olsson C-O, Mischler S. Adsorption of BSA on Passivated CoCrMo PVD Alloy: An EQCM and XPS Investigation. J Electrochem Soc. 2014; 161:294–301.
80. Milošev I. The effect of biomolecules on the behavior of CoCrMo alloy in various simulated physiological solutions. Electrochimica Acta. 2012; 78:259–273.

81. Martin EJ, Pourzal R, Mathew MT, Shull KR. Dominant role of molybdenum in the electrochemical deposition of biological macromolecules on metallic surfaces. Langmuir. 2013; 29:4813–4822. [PubMed: 23550942]
82. Ithurbide A, Frateur I, Galtayries A, Marcus P. XPS and flow-cell EQCM study of albumin adsorption on passivated chromium surfaces: Influence of potential and pH. Electrochim Acta. 2007; 53:1336–1345.
83. Vieira AC, Rocha LA, Papageorgiou N, Mischler S. Mechanical and electrochemical deterioration mechanisms in the tribocorrosion of Al alloys in NaCl and in NaNO3 solutions. Corrosion Science. 2012; 54:26–35.
84. Yan Y, Neville A, Dowson D, Williams S, Fisher J. Effect of metallic nanoparticles on the biotribocorrosion behaviour of Metal-on-Metal hip prostheses. Wear. 2009; 267:683–688.
85. Papageorgiou N, Mischler S. Electrochemical simulation of the current and potential response in sliding tribocorrosion. Tribol Lett. 2012; 48:271–283.
86. Wimmer MA, Loos J, Heitkemper M, Fischer A. The Acting Wear Mechanisms on Metal-On-Metal Hip Joint Bearings – In-Vitro Results. Wear. 2001; 250:129–139.
87. Pourzal R, Theissmann R, Williams S, Gleising B, Fisher J, Fischer A. Subsurface changes of a MoM hip implant below different contact zones. Journal of the Mechanical Behavior of Biomedical Materials. 2009; 2:186–191. [PubMed: 19627822]
88. Pourzal R, Theissmann R, Morlock M, Fischer A. Micro-structural alterations within different areas of articulating surfaces of a metal-on-metal hip resurfacing system. Wear. 2009; 267:689–694.
89. Pourzal R, Theissmann R, Gleising B, Williams S, Fischer A. Micro-structural alterations in MoM hip implants. Materials Science Forum. 2009; 638–642:1872–1877.
90. Wimmer MA, Fischer A, Buscher R, Pourzal R, Sprecher C, Hauert R, Jacobs JJ. Wear mechanisms in metal-on-metal bearings: the importance of tribochemical reaction layers. Journal of Orthopaedic Research. 2010; 28:436–443. [PubMed: 19877285]
91. Pourzal R, Catelas I, Theissmann R, Kaddick C, Fischer A. Characterization of wear particles generated from CoCrMo alloy under sliding wear conditions. Wear. 2011; 271:1658–1666. [PubMed: 21804652]
92. Liao Y, Pourzal R, Wimmer MA, Jacobs JJ, Fischer A, Marks LD. Graphitic Tribological Layers in Metal-on-Metal Hip Replacements. Science. 2011; 334:1687–1690. [PubMed: 22194573]
93. Rainforth WM, Zeng P, Ma L, Valdez AN, Stewart T. Dynamic surface microstructural changes during tribological contact that determine the wear behaviour of hip prostheses: metals and ceramics. Faraday Discussions. 2012; 156:41–57. [PubMed: 23285621]
94. Fischer, A., Williams, S. Self-mating metal articulations in the hip joint. In: ane, Y-WC., Wang, Q., editors. Encyclopedia of Tribology. Springer; USA: 2013. p. 3053-3063.
95. Stickel, D., Fischer, A. The Influence of Topography on the Specific Dissipated Friction Power in Ultra-Mild Sliding Wear: Experiment and Simulation; 2nd. Int. Brazilian Conf. on Tribology – TriboBR-2014; Foz do Iguaçu – Parana – Brazil. 2014.
96. Stickel D, Fischer A. The Alteration of Micro-Contact Parameters during Run-In and their Effect on the Specific Dissipated Friction Power. Tribol Int. 2015; 82:287–296.
97. Catelas I, Medley JB, Campbell PA, Huk OL, Bobyn JD. Comparison of in vitro with in vivo characteristics of wear particles from metal-metal hip implants. Journal of Biomedical Materials Research – Part B Applied Biomaterials. 2004; 70:167–178.
98. Catelas I, Campbell PA, Bobyn JD, Medley JB, Huk OL. Wear particles from metal-on-metal total hip replacements: Effects of implant design and implantation time. Proceedings of the Institution of Mechanical Engineers, Part H: Journal of Engineering in Medicine. 2006; 220:195–208.
99. Billi F, Benya P, Kavanaugh A, Adams J, McKellop H, Ebramzadeh E. The John Charnley award: An accurate and extremely sensitive method to separate, display, and characterize wear debris part 2: Metal and ceramic particles. Clinical Orthopaedics and Related Research. 2012; 470:339–350. [PubMed: 21932105]
100. Guadalupe S, Falcand C, Chitty W, Mischler S. Tribocorrosion in Pressurized High-Temperature Water: A Mass Flow Model Based on the Third-Body Approach. Tribology Letters. 2016; 62:10.

101. Ea HK, Chobaz V, Nguyen C, Nasi S, van Lent P, Daudon M, Dessombz A, Bazin D, McCarthy G, Jolles-Haeberli B, Ives A, Van Linthoudt D, So A, Liote F, Busso N. Pathogenic Role of Basic Calcium Phosphate Crystals in Destructive Arthropathies. Journal Plos one. 2013; 8:1–8.

102. Mischler, S. Sliding Tribo-Corrosion of Passive Metals: Mechanisms and Modeling. In: Peter, B.Jean-Pierre, C.Dirk, D., Friedrich, F., editors. Tribo-Corrosion Res Testing Appl. ASTM international; 2013. p. 1-18.

103. Mathew MT, Nagelli C, Pourzal R, Fischer A, Laurent MP, Jacobs JJ, Wimmer MA. Tribolayer formation in a Metal-on-Metal (MoM) hip joint: an electrochemical investigation. J Mech Behav Biomed Mater. 2014; 29:199–212. [PubMed: 24099949]

Figure 1.
Typical morphology of a McKee-Farrar Hip Joint explant [35]

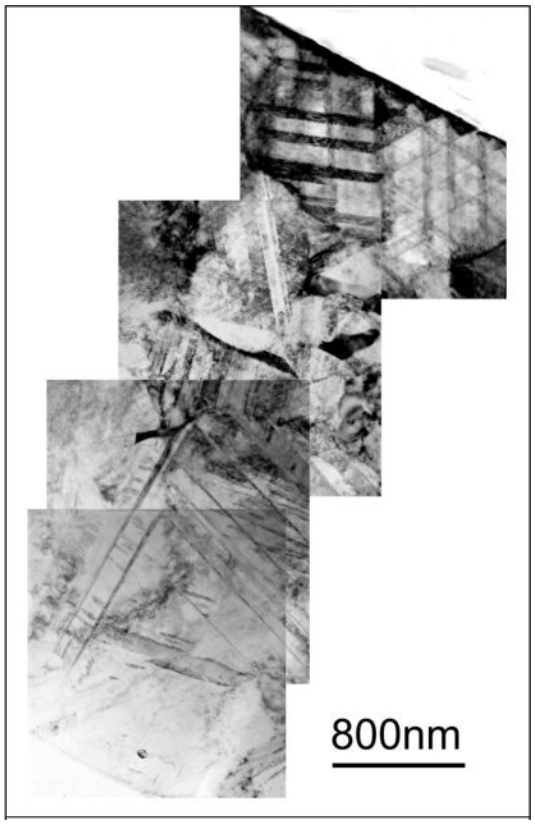

Figure 2.
TEM-Figure of the Strain Gradient characterized by increasing Density of Lattice defects becoming Domains towards the Worn Surface (Wrought HCCoCrMo, FIB-Cut by P. Zeng. M. Rainforth, Sheffield University, UK) [56]

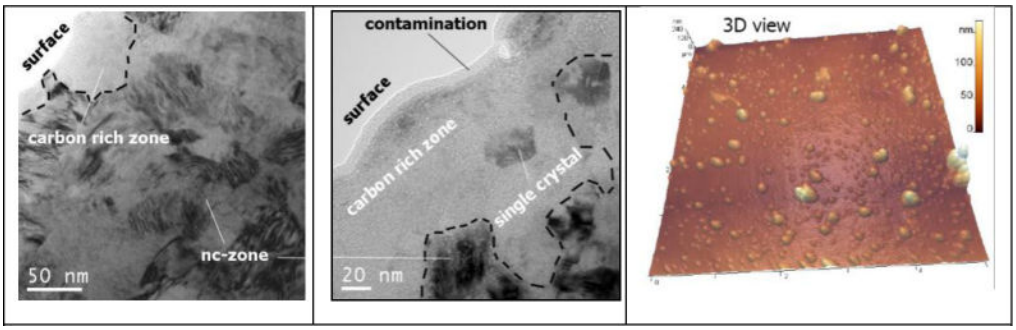

Figure 3.

TEM-micrographs and AFM-Scan of Mechanically Mixed Nanostructured Composite of Residues from Denatured Proteins and Nanometer-Size Wear Particles [56] (AFM-Scan by S. Vasnyov, S. Speller, Radboud University, Nijmegen, The Netherlands)

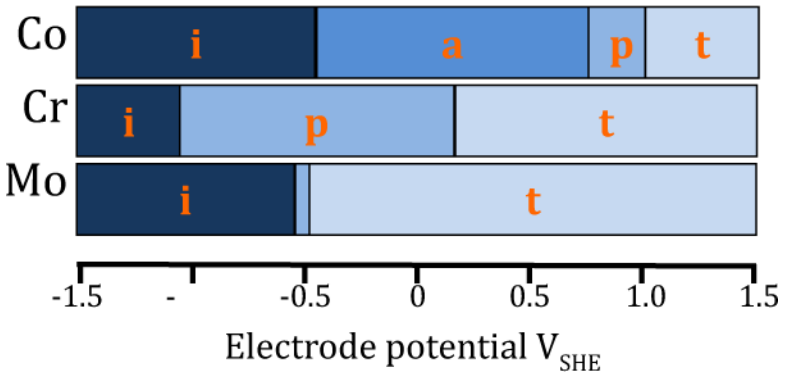

Figure 4.

Theoretical potential ranges for immunity (i), active dissolution (a), passivity (p) and transpassivity (t) of Co, Cr and Mo taken from Pourbaix diagrams at pH 7.4 [72].

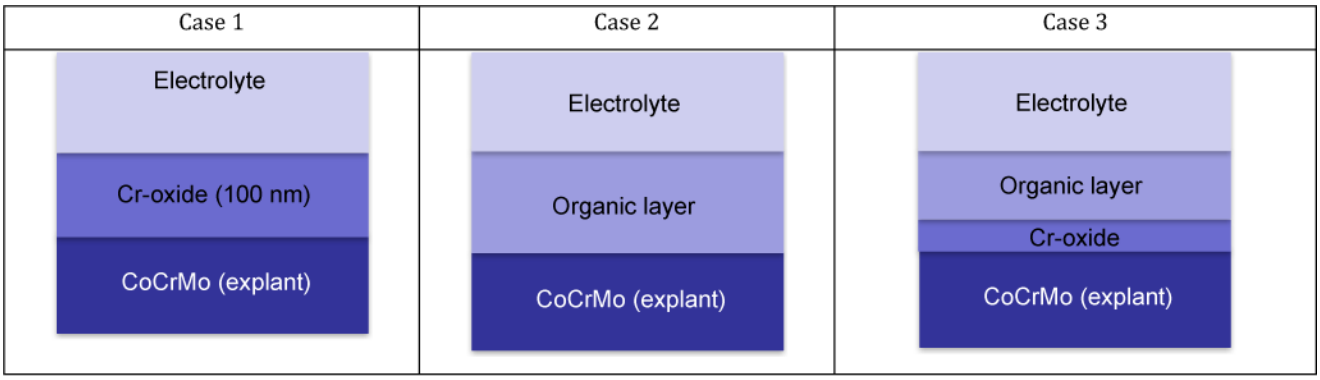

Figure 5.
Schematic view of the three cases of surface reaction film reported in literature.

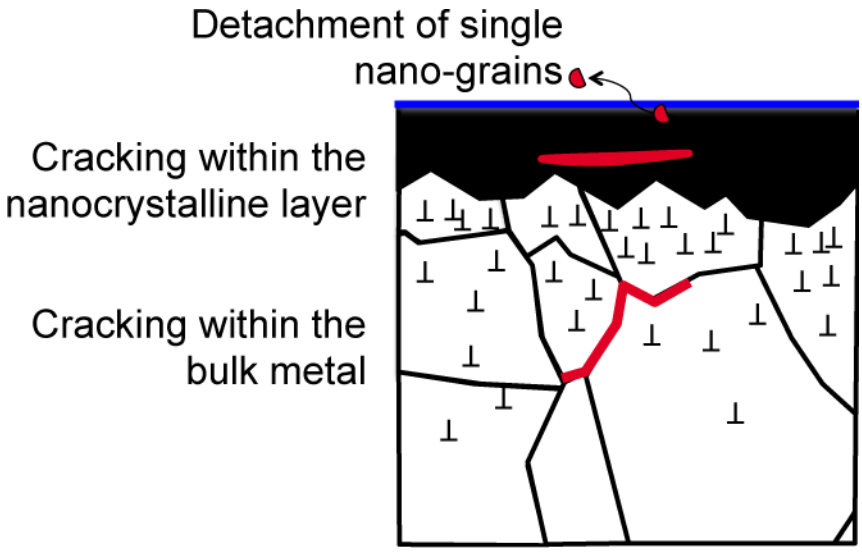

Figure 6.
Scheme showing the possible mechanism of wear particle generation. Adapted from ASTM [102].

Table 1

Synopsys on published data concerning surface transformations and tribomaterial generation in MoM.

Ref	Test conditions, environment	Contacting materials and pressure	Observations SRF = Surface reaction films, MT = Metallurgical transformations, PA = Particle analysis
[86]	In-vitro, Calf serum	Selfmated ISO 5832–12 wrought CoCrMo	**SRF**: Elements detected by EDS C, Na, Cl, K, Cr, Co, Mo, N, O, P, Ca.
[9]	In-vivo	Selfmated ASTMF75 CoCrMo	**SRF**: Thick oxide film by XPS as opposed to the thin passive film observed in the non contact zone.
[87]	In-vitro, Bovine serum	Selfmated ASTM F1537 CoCrMo	**SRF**: EDS-TEM shows C rich layer covering both the contact and non-contact zone. **MT**: In the non-contact zone: Nanocrystalline layer of 100–150 nm thickness and grain size <15 nm. Below the nanocyrstalline layer ε-martensite was observed. In the contact zone a nanocrystalline layer of 200 nm thickness and grain size 35–40 nm.
[88]	In-vivo	Selfmated ASTMF1537 CoCrMo (Hip resurfacing)	**SRF**: EDS-TEM shows carbonaceous layer in the contact zone **MT**: Polishing wear area: Nanocrystalline layer 250–400 nm thickness, grain size 25–50 nm. Scratched area: Nanocrystalline layer 100–150 nm thickness, grain size 15–35 nm. Below the nanocyrstalline layer ε-martensite
[89]	In-vitro (simulator), Bovine Serum	Selfmated ASTMF1537 CoCrMo	**SRF**: EDS-TEM shows 50 nm carbonaceous layer with some mechanical mixing with the alloy **MT**: Similar pattern as in-vivo see previous reference [80]
[90]	In-vivo	Low Carbon ASTM F75	**SRF**: XPS shows 120 nm carbonaceous layer direct on the metal without intermediate oxide film. In the contact zone and a passive film with adventitious C
[91]	In-vitro (lab test), Calf serum	Selfmated HC wrought CoCrMo, 135 MPa	**MT**: Nano-crystalline subsurface zone prior and after test **PA**: Non oxidized metal particles of 300–800 nm length and 100–300 nm width with HCP ε-martensite structure.
[91]	In-vitro (hip simulator), Calf serum	Selfmated HC wrought CoCrMo, 30 MPa	**PA**: Oxidized CoCr particles of 30–80 nm size of two types (I: amorphous containing O, Co, Cr and Mo, II: crystalline containing only Cr and O). Smaller (5–15 nm) Cr_2O_3. particles, type III, were found flaking of from type II
[92]	In-vivo	Selfmated CoCrMo (Hip resurfacing)	**SRF**: Graphitic material layer observed by EELS
[93]	In-vivo	Selfmated forged HC-CoCrMo (Hip resurfacing)	**SRF**: High wear region locally 10 nm thick carbonaceous layer **MT**: Two contact regions: low wear region with 70–150 nm nano-crystalline layer and high wear region with 30nm nano-crystalline layer only locally formed.
[94]	In-vitro (hip simulator), Bovine Serum	Selfmated CoCrMo	**SRF**: EDS shows a 50 nm C layer on a 5–10 nm chromium oxide
[48]	In vitro (Pin-on-disc), Bovine Serum	HC-CoCrMo vs. Alumina	**SRF**: EELS shows 0 to 500 nm thick carbonaceous layer **MT**: Nanocrystalline layer of 0 to 600 nm thickness